Journal of Fusion Energy, Vol. 12, No. 3, 1993

Initial High Beta Operation of the HBT-EP Tokamak

M. K. Vijaya Sankar, E. Eisner, A. Garofalo, D. Gates, T. H. Ivers, R. Kombargi, M. E. Mauel, D. Maurer, D. Nadle, G. A. Navratil, and Q. Xiao[1]

HBT-EP is a new research tokamak designed and built to investigate passive and active feedback techniques to control MHD instabilities. In particular, HBT-EP will be able to test techniques to control fast MHD instabilities occurring at high Troyon-normalized beta, $\beta_N \equiv \beta Ba/I_p$ *[Tm/MA],* since it is equipped with a thick, close-fitting, and adjustable conducting shell. The major goals of the initial operation of HBT-EP have been the achievement of high beta operation (β_N~3) using only ohmic heating and the observation of MHD instabilities. By using a unique fast start-up technique, we have successfully achieved these goals. A variety of MHD phenomena were observed during the high beta operation of HBT-EP. At modest beta ($\beta_N \leq 2$), discharges have been maintained for more than 10 msec, and these discharges exhibit saturated resistive instabilities. When β_N approaches 3, major disruptions occur preceded by oscillating, growing precursors. During start-up, one or more minor disruptions are usually observed. A 1-D transport code has been used to simulate the evolution of the current profile, and these early minor instabilities are predicted to be double tearing modes. The simulation also reproduces the observed high beta operation when saturated neo-Alcator energy confinement scaling is assumed.

KEY WORDS: High beta operation; HBT-EP tokamak.

1. INTRODUCTION

The high beta operation of a tokamak is limited by the occurrence of MHD instabilities that can be classified as: low-n external modes, low-n internal modes, and high-n internal ballooning modes. The low-n external kink mode is predicted to appear at beta values above the Troyon beta limit,[1]

$$\beta \lhd \beta_c \equiv 10^{-8} \frac{C_T I_p}{aB_0} \% \qquad (1)$$

where I_p(A) is the toroidal plasma current, B_0(T) is the vacuum toroidal magnetic field on axis, u(m) is the plasma radius, and C_T is a factor equal to about 3. For the low-n internal mode,[2] the stability limit is more difficult to characterize. In general, the conditions which favor the instability of these modes is the existence of finite pressure gradients in regions of low magnetic shear typically found in the core region of the discharge. Based on the Generomak study,[3] operation of a fusion reactor in the second stability regime at useful fusion power densities using conventional super conducting magnet technology limited to 12 Tesla, requires operation significantly above the Troyon beta limit. For a tokamak plasma stable to high-n ballooning and low-n internal modes, the appearance of the low-n external kink modes places the ultimate constraint on high beta operation.

Although significant progress has been made in the understanding of beta-limiting, low-n modes, very little has been done in controlling these instabilities. Experiments on HBT,[4] PBX,[5] and DIII-D[6] have reported the observation of beta limits in agreement with the prediction of the onset of external kink modes. Because of

[1]Department of Applied Physics, Columbia University, New York, New York 10027.

0164-0313/93/0900-0303$07.00/0

the extremely rapid growth rate of these instabilities, the use of a nearby conducting wall provide the most likely method of stabilizing these modes. The PBX-M[7] uses a close fitting conducting shell with a bean-shaped cross-section plasma. The HBT-EP tokamak has been built to investigate this important area of low-n MHD mode control of beta-limiting phenomena.

The present paper gives the initial results from the HBT-EP tokamak, showing successful achievement of high beta ($\beta_N \simeq 3$) ohmic operation. A comparison of the experimental data and the numerical results obtained from a 1-D transport code is also presented in this paper. This comparison has assisted in the interpretation of the observed MHD perturbations by providing a description of the current profile evolution.

2. DESCRIPTION OF HBT-EP TOKAMAK

HBT-EP, High Beta Tokamak-Extended Pulse, is an upgrade to the HBT tokamak at Columbia University.(*) The ohmically-heated, high β_N operating regime of HBT-EP has been extended to higher temperatures and longer pulse durations than was possible in the previous HBT experiments. HBT-EP makes use of the toroidal field coils from the CLEO tokamak/stellarator built at Culham laboratories,(') a fast ohmic heating system capable of rapid discharge startup and sustained high loop voltage, a flexible poloidal field coil system, and a modular vacuum vessel with good diagnostics access.

The top view of the HBT-EP tokamak is shown in Fig. 1. Twenty toroidal field (TF) coils are grouped into ten coil pairs, and each coil pair is linked by one stainless-steel vacuum chamber segment. This modular arrangement allows easy assembly of the tokamak since each coil pair can be handled separately. The ten vacuum segments, which make up the toroidal chamber, are connected by five quartz insulating breaks, three stainless-steel spool pieces and two bellows sections. In order to achieve the low impurity levels (< 0.2% oxygen) required for high beta ohmic operation, considerable effort was spent in the design of the HBT-EP vacuum system. All vacuum seals are made either with copper gaskets or double o-ring viton seals. Each vacuum chamber segment is surrounded by an insulating heating pad for baking to 110°C, and base pressures as low as 10^{-8} Torr have been achieved.

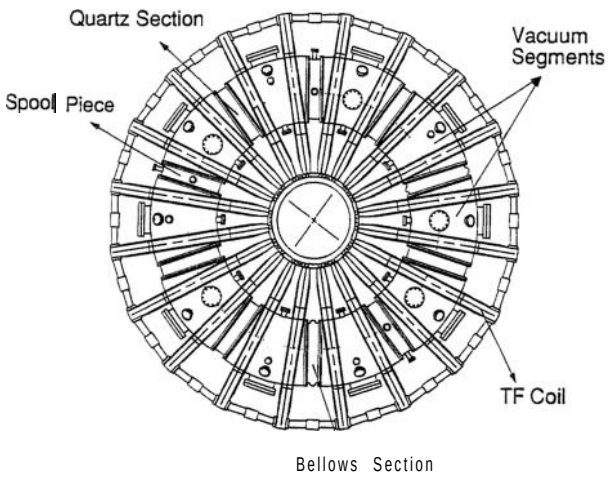

Fig. 1. Top view of the HBT-EP tokamak.

Figure 2 shows the cross-section of HBT-EP. The poloidal field (PF) coil set consists of a six turn ohmic heating (OH) coil (OH1-OH3) and a five turn vertical field (VF) coil (VF1-VF2) The three turn VF2 is anti-parallel to the two turn VF1 and this VF coil has been designed to eliminate the mutual inductance between the OH and VF coil. The air-core ohmic heating coil has been designed to minimize the poloidal field within the plasma and allows fast start-up. The vacuum vessel has been designed to accommodate the installation of a multi-turn shaping coil system, within the bore of the TF magnets, which can be used to produce dee-shaped and diverted discharges. The formation of dee-shaped and diverted discharges have been simulated[10] using the TSC code.[11]

An unique feature of HBT-EP is its adjustable conducting shell. Each vacuum chamber segment contains an upper and lower conducting shell section (see Fig. 2) which covers 26" of the toroidal circumference, thus providing 260" total coverage. The shells are made from spun aluminum, approximately lcm thick, and they are nickel plated to reduce sputtering. Two sets of movable stainless-steel rail limiters (not shown in the figure) determine the size of the plasma.

The OH, VF, and TF coils are powered by capacitor banks. To initiate a typical plasma discharge, the air-core OH transformer is charged with a negative bias current (bias bank) with a rise time of about 500 μsec followed by a fast start current (start bank) with a rise time of about 150 μsec enabling formation of the plasma discharge faster than the magnetic diffusion time. The sustainment of the loop voltage is done by a one Farad electrolytic power crowbar. A low power electron gun is used to provide free electrons to aid in initiating plasma formation. The VF bank (consisting of a fast start followed by power crowbar) is fired at the same time as the OH start bank. The toroidal field is powered by a

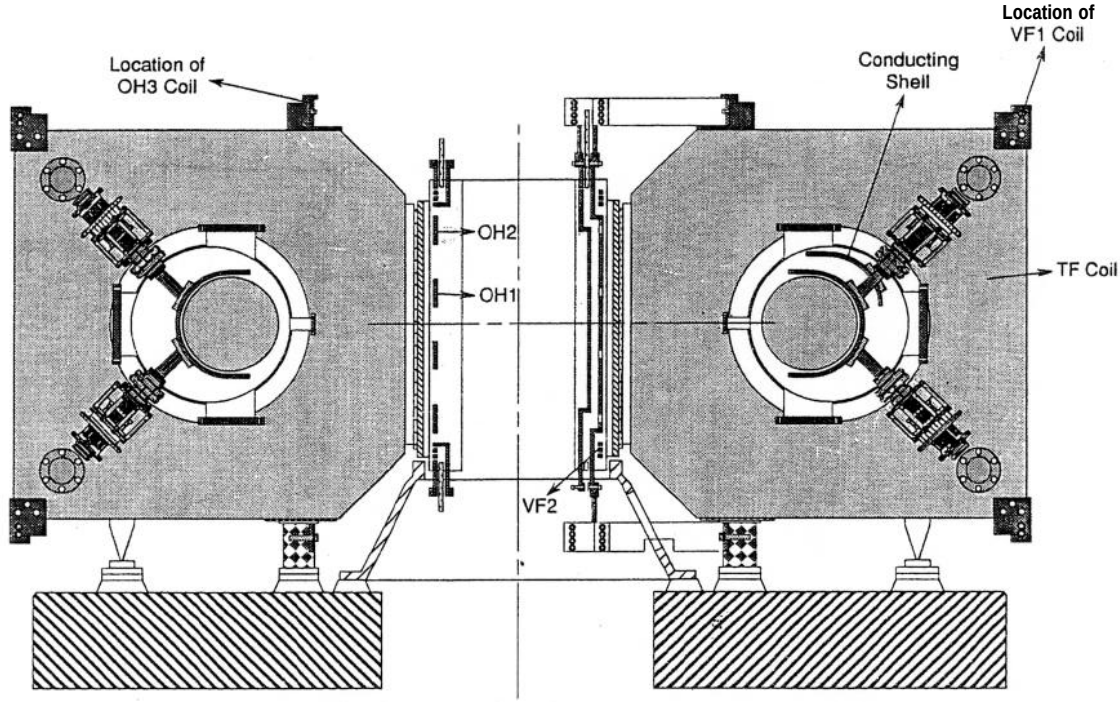

Fig. 2. Cross-section of the HBT-EP tokamak.

2MJ bank with a 100 ms rise time which can generate a maximum of 5.5 kG on axis. The device operates reliably and the shot-to-shot reproducibility of the discharge characteristics is very good.

The diagnostics capability of HBT-EP includes Thomson scattering, CO_2 laser interferometer, magnetic diagnostics, wide-band radiometer, and visible spectroscopy.

3. NUMERICAL MODEL FOR THE HBT-EP DISCHARGES

A 1-D transport code, HERMES[12] along with 0-D calculations have been used to determine the amount of impurity that can be tolerated in HBT-EP, allowing operation with temperature $\sim$100 eV and a value of $\beta_N \simeq 3$. In HERMES, the plasma current is a given constant value. The code has been modified to include the ionization equation for simulating the formation of the discharge. The modified equations are given below.

$$\frac{\partial n_h}{\partial t} = \frac{1}{r}\frac{\partial}{\partial r}\left(rD\frac{\partial n_h}{\partial r}\right) + \nu_{\text{ion}} n_e \qquad (2)$$

$$\frac{\partial n_{\text{imp}}}{\partial t} = \frac{1}{r}\frac{\partial}{\partial r}\left(rD\frac{\partial n_{\text{imp}}}{\partial r}\right) + S_{\text{imp}} \qquad (3)$$

$$\frac{\partial n_n}{\partial t} = -\nu_{\text{ion}} n_e + S_n \qquad (4)$$

$$\frac{3}{2}\frac{\partial}{\partial t}(n_e T_e) = \frac{1}{r}\frac{\partial}{\partial r}\left(r\chi_e \frac{\partial}{\partial r}(n_e T_e)\right) + \frac{J^2}{a} - \nu_{\text{ion}} I n_e - W_{\text{eq}} - W_{\text{rad}} \qquad (5)$$

$$\frac{3}{2}\frac{\partial}{\partial t}(n_i T_i) = \frac{1}{r}\frac{\partial}{\partial r}\left(r\chi_i \frac{\partial}{\partial r}(n_i T_i)\right) + W_{\text{eq}} \qquad (6)$$

$$\mu_0 \frac{\partial}{\partial t}(\sigma E_z) = \frac{1}{r}\frac{\partial}{\partial r}\left(r\frac{\partial E_z}{\partial r}\right) \qquad (7)$$

$$J_z = \sigma E_z \qquad (8)$$

Cylindrical circular geometry is used here. This is a reasonable assumption for a high aspect ratio tokamak like HBT-EP. χ and D are the thermal diffusion and particle diffusion coefficients respectively. Neo-Alcator model is used for the electron energy transport and ion energy transport is neo-classical. Subscripts e, h, imp, i, and n refer to electron, deuterium ion, impurity atom, total ion, and neutral deuterium atom respectively. S_{imp} is the source of sputtered impurity atom from the wall and is assumed to be a given fraction of the deuterium ion flux reaching the wall. The impurity charge state and radia-

tion is evaluated using the average ion corona model given by Post.[13] Neutral deuterium atoms are transported and deposited within the plasma using a Monte-Carlo method. S_n is the corresponding source term. The flux is continually adjusted so that the ionization just balances the loss of deuterium ions by diffusion (a recycling coefficient of unity). J is current density, I is the energy loss due to ionization and exitation of deuterium and is taken to be 40eV, W_{eq} is the equipartition energy, υ_{ion} is the ionization frequency, and σ is the plasma conductivitywith the trapped particle correction included. W_{rad} is the radiation energy and consists of impurity radiation and bremsstrahlung. The initial profiles are assumed to be uniform. The initial deuterium ion density was set at a given fraction (10%) of the initial neutral density, and this density was adjusted to give the best agreement between simulation and experiment. The actual value used corresponded to twice the fill pressure measured in the absence of plasma.

The boundary condition for the electric field is given by

$$\frac{V(t) - E(a,t)2\pi R_0}{L_p} = \frac{2\pi a}{\mu_0}\frac{\partial}{\partial r}E_z(a) \qquad (9)$$

L_p is the plasma inductance, $V(t)$ is the applied loop voltage and the value for a given plasma shot can be calculated as

$$V(t) = M_{oh,pl}\frac{d}{dt}I_{oh} + M_{vf,pl}\frac{d}{dt}I_{vf} \qquad (10)$$

where, $M_{oh,pl}$ and $M_{vf,pl}$ are the mutual inductances between the OH coil and plasma, and the VF coil and plasma respectively. I_{oh} and I_{vf} are the currents through the OH and VF coils respectively. This value of $V(t)$ has been found to agree with the vacuum loop voltage measurement using a flux loop.

In the initial stages of a tokamak discharge, there is possibility for the formation of non-monotonic current profile[14] leading to double tearing mode. The double tearing mode has been included in the modified HERMES following the treatment given by Dnestrovskii and Kostomarov.[15] The code also solves for **A',** the jump in the logarithmic derivative of the perturbed radial magnetic field at the resonant surface, similar to the calculations done by Hastie *et al.*[16] If **A'** is larger than the critical value, then the plasma is unstable to single helicity tearing mode. For the present set of calculations, the value of the island width was determined as a function of the value of the resonant surface in accordance with the calculations of Caneras *et al.*[17], assuming a parabolic current profile. The density and temperature profiles are then made uniform across the island width.

4. RESULTS AND DISCUSSION

The initial high beta operation of HBT-EP was done with a maximum value of the toroidal magnetic field on axis of 0.3T. Calculations done using HERMES and the O-D mode1 showed the maximum permissible oxygen impurity level to be less than 0.2%.[18] In HBT-EP, this was achieved by a proper conditioning of the vacuum vessel involving discharge cleaning in deuterium, followed by baking.

The value of β_p was computed from the requirement of radial equilibrium force balance. This is then used for determining β and $\Lambda \equiv \beta_p + l_i/2$. A constant value of $l_i = 0.65$ was used for the calculation and this value was representative of those predicted by the HERMES calculations. The parameters used for the radial equilibrium force balance are the measured value of the plasma current, the value of the vertical field evaluated using the measured values of the ohmic and vertical field coil currents, and the plasma position measured using the cosine coil. The average electron temperature was estimated from the loop voltage assuming a constant Z_{eff} of 1.1. A list of the parameters of high β_N ($\equiv 10^8\beta aB_o/I_p$) HBT-EP discharges is shown in Table I.

A plot of the conductivity electron temperature and the value of the central electron temperature measured using Thomson scattering is shown in Fig. 3 as a function of the equivalent puff valve electron density, corresponding to the neutral gas fill pressure. Both the

Table I. Measured and Calculated Parameters of Initial High β_N HBT-EP Discharges

Toroidal magnetic field on axis, B_o	0.3 T
Plasma current, I_p	13.5-32 kA
Plasma current rise time	150 μsec
Discharge duration	≤ 11 ms
Major radius, R_0	0.94 m
Minor radius, a	0.13-0.2 m
Aspect ratio	4.7-7.2
Cylindrical safety factor, q^*	>2
$\Lambda \equiv \beta_p + l_i/2$	≥ 3
Internal inductance (simulated), l_i	0.9
β_N	≃ 3
Conductivity temperature, $\langle T_e \rangle$, assuming $z_{eff} \simeq$ 1.1	30-50 eV
Electron density corresponding to the injected neutral density, n.	1-3 x 10^{19} m^{-3}

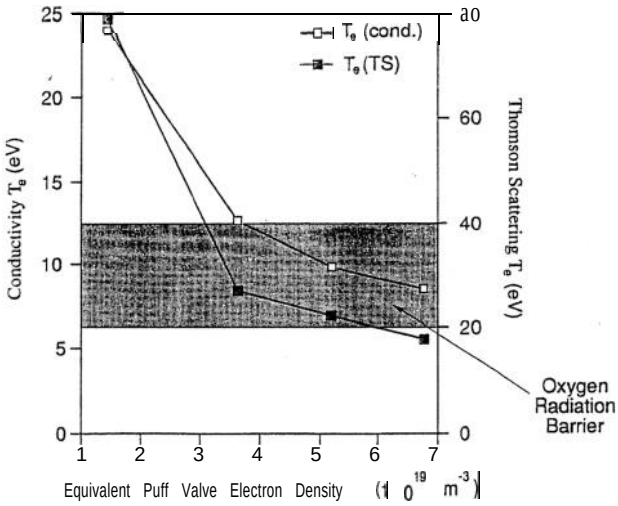

Fig. 3. Comparison of the conductivity electron temperature and the central electron temperature measured using 'Thomson scattering.

conductivity temperature and the Thomson scattering temperature are seen to scale with the equivalent puff valve electron density in a similar way. Also shown shaded in the figure is the approximate oxygen radiation barrier, above which the radiation due to the oxygen impurity decreases rapidly. For electron densities below 3 x 10^{19} m^{-3}, HBT-EP is seen to be capable of crossing the oxygen radiation barrier and reaching temperatures of 80 eV.

Figures 4 and 5 give a representative high beta discharge, where the maximum value of β_N was $\simeq$ 3. For this discharge, the conducting shells were fully retracted and located about 5 cm from the plasma surface, and the limiters were located to produce a discharge with a = 0.13 m. The total duration of the discharge was about 3.5 ms. The traces in Fig. 4 show, from top to bottom, (a) the plasma current, (b) the loop voltage, (c) the average electron temperature, (d) β_N, and (e) the output from the cos2θ rogowski coil. The traces (a)-(d) also contain the values obtained from the numerical simulation. Fairly good agreement is seen between the numerical and the experimental results. The plasma current initially rises to about 9.3 kA in about 135 μsec, then drops to about 8.7 kA and rises again to a peak value of about 13.5 kA. At about 2.1 ms, the plasma current shows a sudden rise and then decreases slowly accompanied by some fluctuations before disrupting at 3.4 ms. The loop voltage trace shows a negative spike around 2.1 ms followed by positive fluctuations. This negative voltage spike can be due to tearing mode activity occurring in the plasma.[19] In the numerical simulation, m = 2 double tearing mode is predicted to occur near this time. The output from the cos2θ rogowski coil also show fluctuations around 2.1 ms. The maximum value of the average electron temperature attained for this discharge is seen to be about 30 eV.

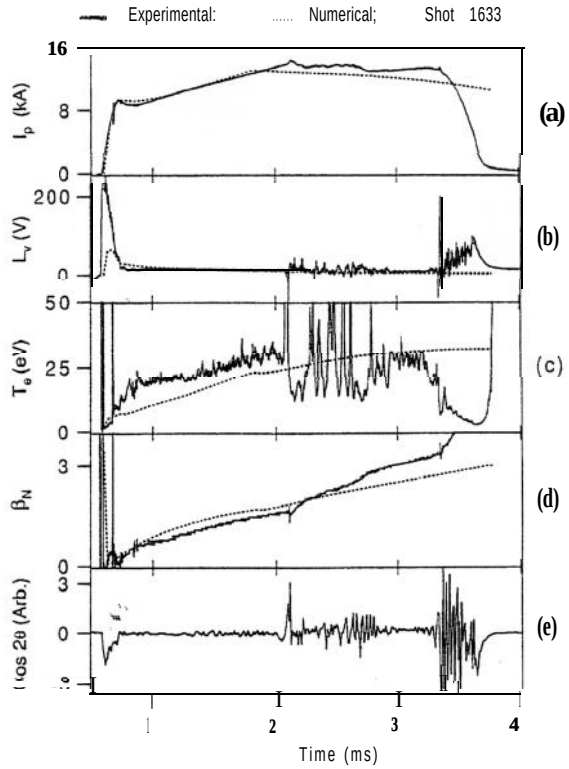

Fig. 4. Time evolution of the plasma parameters for a typical high beta discharge showing (a) plasma current, I_p, (b) loop voltage, L_v, (c) average electron temperature, (T_e), (d) Troyon-normalized beta, β_N, and (e) signal from the cos2θ rogowski coil.

Just before the major disruption at 3.4 ms, the experimental trace of the cos2θ rogowski coil shows oscillations increasing in amplitude. The value of β_N at the time of major disruption was observed to be about 3.2, typical of high beta disruption. By adjusting the neutral fill pressure, HBT-EP can produce low beta discharges ($\beta_N \sim$ 1.5) that has a pulse length of about 11 ms (several energy confinement times). In these discharges, high beta disruptions were not observed, although continuous saturated instabilities were present.

Figure 5 shows the traces, from top to bottom, (a) R_p, the major radius of the plasma current centroid, (b) the value of β, (c) the value of A, (d) the value of cylindrical-q* $\equiv 2\pi a^2 B_o/(\mu_o R_o I_p)$, and (e) the output from a wide-band radiometer. The major radius of the plasma current centroid is seen to be nearly a constant for the

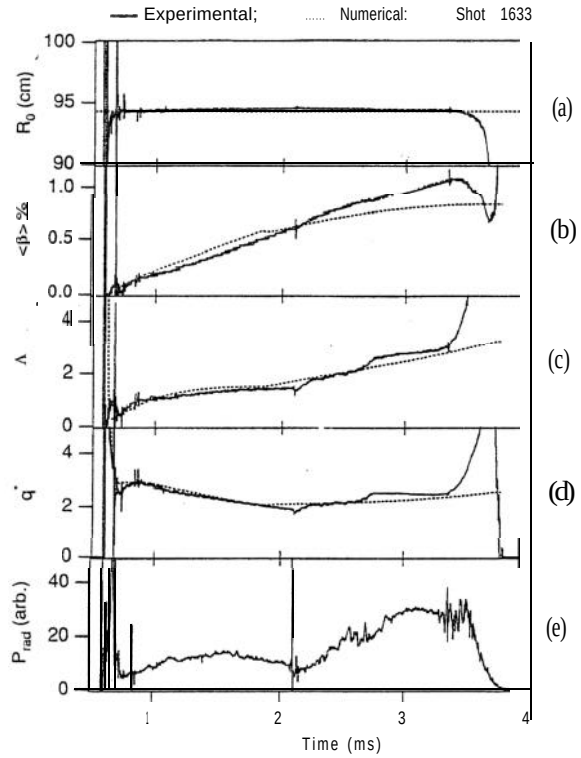

Fig. 5. Time evolution of the plasma parameters for a typical high beta discharge showing (a) major radius, R_0, (b) $\langle\beta\rangle$, (c) A $\equiv \beta_p + l_i/2$, (d) q*, and (e) radiated power from the-plasma.

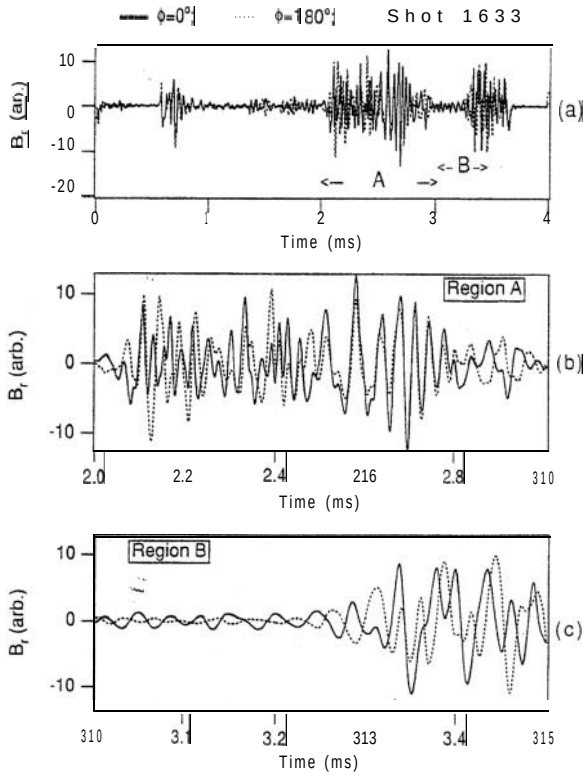

Fig. 6. The outputs from the magnetic pickup coils separated toroidally by 180° (a), with details of region A (b), and region B (c).

duration of the discharge. In the numerical simulation, the major radius has been assumed to be a constant. The maximum value of β reaches about 1% just before the major disruption. The value of q* is close to two for most of the discharge. From the radiometer, it is seen that the radiated power, after the initial spike, slowly increases and then decreases with a quarter period of about 0.75 ms. At about 2.1 ms, the radiated power starts to increase again. This is believed to be due to the influx of neutral deuterium and impurities from the wall following the minor disruptive event. This sudden influx of gas is not modeled in the numerical simulation.

Figure 6 shows the oscillatory part of the radial magnetic field measured by two magnetic pickup coils separated toroidally by 180". The output from the coils has been integrated to obtain the radial magnetic field, and the ocillatory part is obtained by subtracting the time average. The initial oscillatory signal occurring before 0.8 ms corresponds to the discharge formation. Oscillations are seen on the radial magnetic field, occurring when the loop voltage and the cos2θ monitors show fluctuations. The first set of oscillations (region A) damp out at around 2.8 ms. This is then followed by oscillations growing in amplitude with a mode number of n = 1 (region B), just before the disruption Expanded scales of regions A and B are also shown. In region A, there seems to be mixing of an odd mode (n = 1) and an even mode (n = 2). A reduction in frequency is seen just before the oscillations in region A damps out. This is similar to the phenomenon of mode locking seen in other tokamaks.[20] Region B shows the growth of the n = 1 mode just before the disruption.

Figures 7 and 8 show the profiles of the electron temperature and the plasma current density obtained from the numerical simulation. In the initial stages of the discharge, a skin current forms leading to double tearing modes. The maximum value of the electron temperature on the axis is about 60 eV, just before the experimentally observed major disruption. Near this time, the code also predicts the plasma to be unstable to the m = 2 tearing mode. Note, however, that the details of the major disruption are not. modeled in the simulation and we do not have yet any confirmation of m = 2 tearing activity preceding a major disruption.

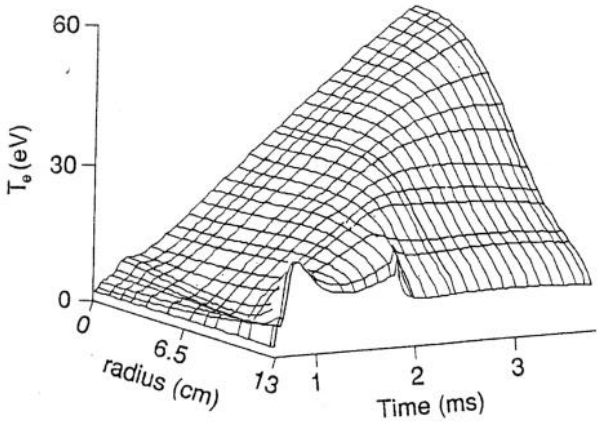

Fig. 7. Electron temperature profile from the numerical simulation.

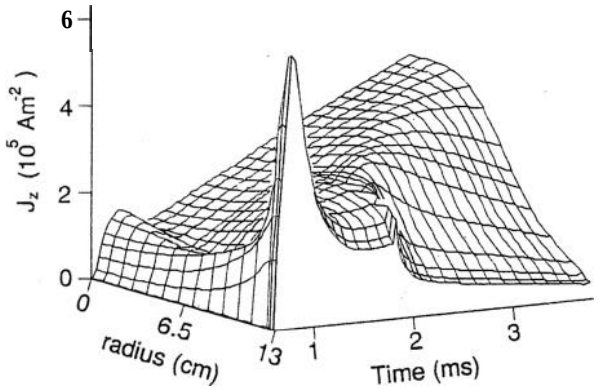

fig. 8. Plasma current density profile from the numerical simulation.

5. CONCLUSIONS

A new research tokamak, HBT-EP, has been built to investigate the MHD instabilities that occur during high beta ($\beta_N \gtrsim 3$) operation. Successful operation of HBT-EP at the design goals has been achieved. A value of $\beta_N = 3$ has been obtained in HBT-EP by using an unique fast current start-up technique.

A variety of MHD activity were observed during the high beta operation of HBT-EP. A major disruption was observed to occur when the value of β_N reached $\simeq$ 3. These disruptions were sometimes preceded by one or more minor disruptions with associated negative spikes on the loop voltage signal. For discharges with $\beta_N \leq 2$, pulse duration $\geq$ 10 ms have been obtained. Saturated resistive instabilities were observed in these low β_N discharges.

A 1-D transport code has been used to simulate the evolution of the HBT-EP discharge. Good agreement is seen between the numerical simulation and the experiment. In the simulation, the plasma current density is predicted to become non-monotonic during the initial stages of the discharge, making the plasma susceptible to the onset of double tearing modes. Double tearing modes were predicted to become unstable near the time, when minor disruptions were observed in the experiment.

ACKNOWLEDGMENTS

We wish to gratefully acknowledge D. Robinson and T. Todd of Culham Laboratory for making available the CLEO toroidal field coils and support structure for use in building HBT-EP. We also wish to thank M. H. Hughes for supplying the HERMES code, and S. Jardin for supplying and J. DeLucia for running the TSC code. The technical help of Nick Rivera, Moe Cea and Hank Alvestad during the construction and operation of HBT-EP is greatly acknowledged. This work was supported by the U.S. Department of Energy contract number DE-FG02-86ER53222.

REFERENCES

1. F. Troyon, R. Gruber, H. Sauremnann, S. Semanzato, and S. Succi (1984). ***PLasma Phys. Controlled Fusion 26, 209.***
2. J. Manickam, N. Pomohrev, and A. M. M. Todd (1987). Nucl. ***Fusion 27,*** 1461.
3. J. Sheffield. R. A. Dory, S. M. Cohn. J. G. Delene, L. Parsly, D. E. T. F.'Ashby, and W. T. Reierson (1986). ***Fusion Technol. 9,*** 199.
M. E. Mauel, T. H. Ivers, H. Y. Che, D. Chen, D. Gates, T. C. Marshall, G. A. Navratil, and J. Wang (1989). ***Plasma Physics and Controlled Nuclear Fusion Research 1988, Nice*** (Vol. 1) (International Atomic Energy Agency, Vienna), p. 415.
5. K. Bol, D. Buchenauer, M. Chance, P. Couture, H. Fishman, R. Fonck, G. Gammel, B. Grek, K. Ida, K. Itami, K. Jaehnig, G. Jahns, D. Johnson, R. Kaita, S. Kaye, H. Kugel, B. LeBlanc, J. Manickam, K. McGuire, N. Ohyabu, M. Okabayashi, E. Powell, M. Reusch, G. Schmidt, S. Sesnic, H. Takahashi, and F. Tenney ***(1986). Phys. Rev. Lett. 57,*** 1891.
6. E. J. Strait, L. L. Lao, T. S. Taylor, M. S. Chu, J. K. Lee, A. D. Turnbull, S. L. Allen, N. H. Brooks, K. H. Burrell, R. W. Callis, T. N. Carlstrom, M. S. Chance, A. P. Colleraine, D. Content, J. C. DeBoo, J. Ferron, J. M. Greene, R. J. Groebner, W. W. Heidbrink, F. J. Helton, D. N. Hill, R.-M. Hong, N. Hosogane, W. Howl, C. L. Hsieh, G. L. Jackson, G. L. Jahns, A. G. Kellman, J. Kim, S. Kinoshita, E. A. Lazarus, P. J. Lomas. J. L. Luxon, M. A. Madhavi, Y. Neyatani, T. Ohkawa, T. H. Osborne, D. 0. Overskei, T. Ozeki, M. Perry, P. I. Peterson, T. W. Petrie, J. C. Philips, G. D. Porter, D. P. Schissel, J. T. Scoville, R. P. Seraydarian, M. Schimada, T. C. Simonen, R. T. Snider, R. D. Stambaugh, R. D. Stav, H. St. John, R. E. Stockdale, U. Stroth, and R. Wood (1989). ***Plasma Physics and Con-***

trolled Nuclear Fusion Research 1988, Nice (Vol. 1) (International Atomic Energy Agency, Vienna), p. 83.
7. M. Okabayashi, N. Asakura, R. Bell, S. Bernabel, K. Bol, R. A. Ellis. Jr., R. J. Fonck, G. Garnmel, A. Holland, R. Kaita, S. Kaye, H. W. Kugel, B. LeBlanc, A. MacAulay M. Ono, S. Paul. E. Powell. S. Preische. M. Reusch. S. Sesnic. and H. Takahashi *(1989). Plasma Physics and Controlled Nuclear Fusion Research* 1988, Nice (Vol. 1) (International Atomic Energy Agency, Vienna), p. 97.
8. T. H. Ivers, M. E. Mauel, G. A. Navratil, D. Gates, M. K. Vijaya Sankar, T. C. Marshall, and J. Wang (1991). ***Plasma Physics and Controlled Fusion Research 1990, Washington*** (Vol. 1) (International Atomic Energy Agency, Vienna), p. 573.
9. D. R. Robinson, N. R. Ainsworth, P. R. Collins, A. N. Dellis, T. Edlington, P. Haynes, S. Iyengar, I. Johnson, B. Lloyd, M. O'Brien. B. J. Pasham. A. C. Riviere. D. F. H. Start, and T. N. Todd *(1987) Plasma Physics and Controlled Fusion Research,* 1986, Kyoto (Vol. 1) (International Atomic Energy Agency), p. 575.
10. M. K. Vijaya Sankar, J. DeLucia, M. E. Mauel, and G. A. Navratil (1989). ***Bull. Am. Phys. Soc. 34, 1992.***
11. S. C. Jardin, N. Pomphrey, and J. DeLucia (1986). J. Comp ***Phys.*** 66,481.
12. D. E. T. F. Ashby and M. H. Hughes (1981). Nucl. ***Fusion*** 21, 911.
13. R. V. Jensen, D. E. Post, and D. I. Jassby (1978). Nucl. Sci. ***Eng. 65, 282.***
14. S. V. Mimov and ***I.*** B. Semenov (1978). ***Sov. J. Plasma Phys.*** 4, 27.
15. Y. N. Dnestrovskii and D. P. Kostomamv (1986). in ***Numerical Simulation of Plasmas.*** J. L. Armand, H. Cabannes, M. Holt, H. B. Keller, J. Killeen, S. A. Orszag, and V. V. Rusanov (eds.) (Springer-Verlag, Berlin), pp. 266-274.
16. R. J. Hastie, A. Sykes, M. Turner, and J. A. Wesson (1977). *Nucl.* ***Fusion*** 17,515.
17. B. Carreras, B. V. Waddell, and H. R. Hicks (1979). Nucl. ***Fusion*** 19, 1423.
18. M. K. Viiava Sankar and M. E. Mauel (19901. Columbia University Plasma Physics Laboratory Report No. 119.
19. J. A. Wesson, D. J. Ward, and M. N. Rosenbluth (1990). Nucl. ***Fusion 30,*** 1011.
20. M. F. F. Nave and J. A. Wesson (1990). Nucl. ***Fusion 30,2575.***